Creep of Anisotropic Clay: New Microplane Model

By Zdeněk P. Bažant,[1] F. ASCE, and Pere C. Prat,[2] S. M. ASCE

Abstract: As a simpler alternative to a previous microplane model, a new microplane model is presented, in which the relative slipping of clay platelets is characterized by normal rather than shear strains on the microplanes. As is the case for Batdorf and Budianski's slip theory of plasticity, the microplanes are constrained statically, i.e., the stress components on a microplane are the resolved components of the macroscopic stress, while the previous model used a kinematic constraint. This different type of constraint is needed to model correctly material anisotropy. The distribution function of normal strain rate intensity for microplanes of various orientations is calculated from the frequency distribution function of clay platelet orientations, which was approximately determined by other authors from X-ray diffraction measurements. The 6×6 fluidity matrix is calculated from the principle of complementary virtual work on the basis of deformations of individual microplanes and the current values of the stress components. The activation energy approach, validated in previous works, is used to quantify the dependence of the normal strain rates on the microplanes of all orientations as a function of the stress level and temperature. A numerical algorithm to calculate the fluidity matrix is given, and typical test data from the literature are analyzed. With only two free material parameters, good fits of the data are achieved, including their anisotropic features. The modeling is limited to deviatoric creep, and volumetric response is left for subsequent work. The proposed model could be used in finite element programs.

Introduction

Creep of clays in natural deposits often exhibits significant anisotropy that has arisen through the previous long-time consolidation. The microscopic fabric of such clays is distinctly anisotropic, and microscopic examinations reveal that the frequency distribution of the orientations of the clay platelets is nonuniform. The objective of the present paper is to formulate a constitutive law that is usable in finite element programs.

Each element of the fourth-order three-dimensional incremental fluidity tensor must be defined as a function of the stress tensor. This task is not easy to accomplish without some micromechanics analysis. An attempt along this line was made by Bažant, et al. (9), who based their model on a triangular cell of three clay platelets sliding over each other. Their model, however, was only two-dimensional, although a certain approximate generalization to three dimensions was also proposed.

A truly three-dimensional constitutive model for deviatoric creep of anisotropic clay, based on the activation energy approach, was recently developed by Bažant and Kim (6). Pande and Sharma (22,23) used a similar approach, although without the activation energy concept. These models were analogous to the slip theory of plasticity suggested by Taylor (28) and developed by Batdorf and Budianski (3). In this classical theory, the inelastic deformation is defined independently on planes of various orientations in the material, presently called the microplanes (4,6–8). In addition, the interaction between the microplanes and the macrolevel is assumed to be characterized by an equilibrium (or static) constraint, which requires that the stress components on each microplane are the resolved components of the macroscopic tensor.

The previous model by Bažant and Kim, however, used the opposite assumption, namely that the microplanes are constrained kinematically rather than statically, i.e., the strain components on a microplane of any direction are the resolved components of the macroscopic strain tensor. The original reason for choosing this dual constraint was that a kinematically constrained microstructural model is more stable in numerical analysis, as transpired from the previous formulation of the microplane model for concrete (7,8). However, another, more compelling, reason was the finding that a statically constrained microplane model with shear strains would give an incorrect picture of anisotropy; for the direction in which there are more interparticle slip planes, it would give a lower rather than a higher creep rate. We will nevertheless see that this incorrect anisotropy of the kinematically constrained model is limited to inelastic deformations that arise from shear deformations on the microplanes.

Our purpose in micromechanics modeling is to determine the interaction between inelastic phenomena on planes of various orientations, but not to completely describe the deformations in the microstructure. In particular, we do not attempt to introduce individual particles and the slips among them. Thus, our relationship between the deformations on the microplanes to the actual interparticle slips is essentially phenomenological. In the previous work (6), it was assumed that interparticle slip corresponds to a shear deformation on the microplanes. This is not necessarily so, however. The shear slip between particles may be equally well imagined to result in normal strains on the microplanes, as may be shown for some particle arrangements and movements; see Fig. 1. The reason for the possibility of two different interpretations is the ambiguity in associating the microscopic particle displacements with the deformation of the macroscopic homogenizing continuum.

Adopting in this study the assumption that interparticle slip results in normal strains on the microplanes, we achieve a considerably simpler model than in the previous work (6). In three dimensions, each microplane has infinitely many possible directions of shear strain, but only one direction of normal strain. This simplicity is perhaps the main reason for introducing a new approach.

As already pointed out, the modeling of interparticle slip by shear deformations on the microplanes is limited to the kinematically constrained approach. For a statically constrained microplane model, this would lead again to an incorrect picture of anisotropy; the deformation rate on the planes of an orientation for which there are more interparticle slip planes in the microstructure, the model would predict a smaller rather than a higher creep rate, which would be incorrect. Thus, the statically constrained model appears to be inevitable if the interparticle slip should

[1]Prof. of Civ. Engrg. and Dir., Ctr. for Concrete and Geomaterials, Northwestern Univ., Tech 2410, Evanston, IL 60201.

[2]Grad. Res. Asst., Ctr. for Concrete and Geomaterials, Northwestern Univ., Tech 2410, Evanston, IL 60201.

Note.—Discussion open until December 1, 1987. To extend the closing date one month, a written request must be filed with the ASCE Manager of Journals. The manuscript for this paper was submitted for review and possible publication on May 8, 1986. This paper is part of the *Journal of Engineering Mechanics*, Vol. 113, No. 7, July, 1987. ©ASCE, ISSN 0733-9399/87/0007-1050/$01.00. Paper No. 21648.

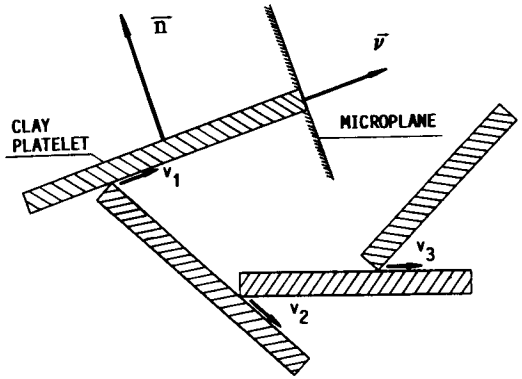

FIG. 1.—Particle Tips with Sliding Velocities v_1, v_2, v_3 Are Assumed to Follow Displacements of Macroscopic Homogenized Continuum

be modeled by normal rather than shear deformations on the microplanes. This might be a source of difficulty if we intended to model strain-softening, for which a kinematic rather than static constraint seems to be necessary for stability reasons. In the present work, however, we do not intend to treat strain softening.

Determination of Fluidity Tensor

We introduce the following basic hypotheses:

1. Only deviatoric deformations are modeled, i.e., the volume change and the hydrostatic pressure effect are ignored.
2. The interparticle slip rate is introduced by means of its equivalent normal deformation rate on a microplane normal to the slip direction.
3. The distribution frequency $\Phi(\boldsymbol{\nu})$ of the normal deformation rates on the microplanes is given (as a function of orientation vector $\boldsymbol{\nu}$).
4. The microplanes are statically rather than kinematically constrained, the same as in the classical slip theory of plasticity (3).
5. The rate of interparticle slipping depends on temperature and stress as indicated by the activation energy concept of the rate process theory (13,15).

The last hypothesis was introduced and partially verified during the 1960s by Christensen (12), Campanella (10,30), Mitchell (17,18,26), and others (19–21,31). However, it was not used in three-dimensional triaxial constitutive relations or micromechanics models until it was formulated in Refs. 6 and 9.

The assumption that the interparticle slipping is modeled as a normal strain rate may be justified if it is assumed that the particle tips follow the macroscopic deformation of the homogenized continuum (Fig. 1). On the other hand, if it were assumed that the particle centroids follow the macroscopic deformation, then this hypothesis would not be appropriate.

According to the hypothesis of a statically constrained microstructure, the components of the stress vector on the microplane are the resolved components of the macroscopic stress tensor; $(\vec{\boldsymbol{\sigma}}_\nu)_i = \nu_j \sigma_{ij}$, in which ν_j = direction cosines of the unit normal to this microplane, imagined to represent the direction of the interparticle slips that are modeled by this microplane; and σ_{ij} = macroscopic stress tensor components. Latin lower case subscripts refer to Cartesian coordinates, x_i (i = 1, 2, 3). Projection of the stress vector $\vec{\boldsymbol{\sigma}}_\nu$ onto the unit normal vector $\vec{\boldsymbol{\nu}}$ yields the normal stress on the microplane:

$$\sigma_\nu = \nu_i \nu_j \sigma_{ij} \quad \text{(1)}$$

According to the rate process theory, which is now generally accepted for the creep of clays, the rate of sliding at interparticle contacts may be expressed as

$$\dot{\epsilon}_\nu = k_1 \sinh (k_2 \sigma_\nu) \quad \text{(2)}$$

in which $\dot{\epsilon}_\nu$ = rate of normal strain for the microplane, imagined to correspond to the rate of interparticle slips in this direction; and

$$k_1 = 2A \left(\frac{kT}{h}\right) t^{-m} e^{-Q/RT} = k_0 t^{-m} \quad \text{(3)}$$

$$k_2 = \frac{V_a}{RT} \quad \text{(4)}$$

where T = absolute temperature; Q = activation energy of interparticle bonds; R = universal gas constant; k = Boltzmann constant; h = Planck constant; V_a = activation volume; A = empirical constant characterizing the number of active bonds for slip in this direction; m = empirical time exponent describing the time decay of the creep rate (the stress being assumed constant); and k_0 = coefficient depending on temperature.

To determine the compatibility relation between the microstrain rates on the individual microplanes and the macroscopic strain-rate tensor, the principle of complementary virtual work may be used. This principle requires that the complementary virtual work done by the macrostrain rates within a sphere of unit radius be equal to the complementary virtual work done by all the microstrain rates on the microplanes of all orientations:

$$\delta W = \frac{4\pi}{3} \dot{\epsilon}_{ij} \delta \sigma_{ij} = 2 \int_S \dot{\epsilon}_\nu \delta \sigma_\nu \Phi(\boldsymbol{\nu}) dS \quad \text{(5)}$$

in which $4\pi/3$ represents the surface of a unit sphere. The factor 2 is introduced because the integration needs to be carried out only over the surface S of a unit hemisphere, since the integrand values at two diametrically opposite points are the same; $\Phi(\boldsymbol{\nu})$ is the given distribution function for the frequency of the slip directions associated with various microplanes of unit normals $\boldsymbol{\nu}$.

Substitution of Eqs. 1 and 2 into Eq. 5 yields

$$\frac{4\pi}{3} \dot{\epsilon}_{ij} \delta \sigma_{ij} = 2 \int_S k_1 \sinh (k_2 \sigma_\nu) \nu_i \nu_j \delta \sigma_{ij} \Phi(\boldsymbol{\nu}) dS \quad \text{(6)}$$

Noting that $\delta\sigma_{ij}$ may be moved in front of the integral in Eq. 6, and that Eq. 6 must hold for arbitrary stress variations, $\delta\sigma_{ij}$, we conclude that

$$\frac{4\pi}{3}\dot{\epsilon}_{ij} = 2\int_S k_1 \sinh(k_2\sigma_\nu)\nu_i\nu_j\Phi(\boldsymbol{\nu})dS \quad (7)$$

It is now convenient to introduce inside the integrand the factor $\sigma_\nu/\nu_k\nu_m\sigma_{km}$, which equals 1:

$$\frac{4\pi}{3}\dot{\epsilon}_{ij} = 2\int_S k_1 \sinh(k_2\sigma_\nu)\nu_i\nu_j\frac{\nu_k\nu_m\sigma_{km}}{\sigma_\nu}\Phi(\boldsymbol{\nu})dS \quad (8)$$

Again, σ_{km} may be brought outside the integral since it is independent of direction $\boldsymbol{\nu}$. This yields

$$\dot{\epsilon}_{ij} = \left[\frac{3}{2\pi}\int_S \nu_i\nu_j\nu_k\nu_m\frac{k_1\sinh(k_2\sigma_\nu)}{\sigma_\nu}\Phi(\boldsymbol{\nu})dS\right]\sigma_{km} \quad (9)$$

This equation may be rewritten as

$$\dot{\epsilon}_{ij} = \beta_{ijkm}\sigma_{km} \quad (10)$$

in which β_{ijkm} = fourth-order tensor of the current fluidities, which represents the inverse of the viscosity tensor and is defined as

$$\beta_{ijkm} = \frac{3}{2\pi}\int_S \nu_i\nu_j\nu_k\nu_m\frac{k_1\sinh(k_2\sigma_\nu)}{\sigma_\nu}\Phi(\boldsymbol{\nu})dS \quad (11)$$

As mentioned before, we attempt in this paper to model only the deviatoric creep of clay. The volumetric creep represents a more difficult question that requires dealing with its coupling to the deviatoric deformations and probably necessitates introduction of the key features of the critical state theory of soil plasticity. Consideration of these aspects is beyond the scope of the present study and is planned for a subsequent funding period.

Since σ_{ij} is required to be the deviatoric part of the stress tensor, there is no need to make a distinction between the total stress and the effective stress, which takes into account the effect of pore pressure. The deviatoric effective and total stress components are the same, regardless of pore water pressure. As for the strain rate tensor $\dot{\epsilon}_{ij}$, likewise only its deviatoric components are predicted by the present formulation.

Numerical Solution

In practical applications, the integral in Eq. 11 has to be evaluated numerically. It may be approximated by the finite sum

$$\beta_{ijkm} = 6\sum_{\alpha=1}^{n} w_\alpha\left[\nu_i\nu_j\nu_k\nu_m\frac{k_1\sinh(k_2\sigma_\nu)}{\sigma_\nu}\Phi(\boldsymbol{\nu})\right]_\alpha \quad (12)$$

in which subscripts α refer to the integration points on the surface of the unit hemisphere at which the integrand is evaluated; and w_α = the weights (coefficients) of the numerical integration formula, such that $\Sigma_\alpha w_\alpha = 0.5$ for the hemisphere. McLaren's integration formula (5,8,27), which

involves 25 integration points per hemisphere and is of eleventh degree (i.e., integrates exactly an eleventh-degree polynomial on the sphere surface) is used in all the present calculations. For axisymmetric stress states, many of the integrated values are equal, and the formula can then be reduced to only six integration points. Other integration formulas, which are more accurate but use more integration points, or have some other special advantages, are listed in Ref. 8 and derived in Ref. 5.

When all the stress components are prescribed and no conditions are imposed on the strain rates, Eqs. 10–11 can be simply evaluated to obtain the strain rates for given stresses. However, this is not the case in simulating typical laboratory tests. For the tests of deviatoric (shear) creep, the strain rates must satisfy the condition of constancy of volume, and the values of the lateral stresses are unspecified and depend on this condition. Therefore, a more complicated numerical algorithm is required to obtain the strain rates and lateral stresses for a prescribed axial stress. One must use small increments of axial stress to reach the prescribed axial stress level gradually, thus being able to follow the dependence of strain rates and lateral stresses on the axial stress. This has been done according to the following algorithm:

1. Input k_0, k_2, $\Phi(\boldsymbol{\nu})_\alpha$, w_α, t, m, and the tolerance for iterations. Evaluate $k_1 = k_0 t^{-m}$. Calculate coefficients $\nu_i\nu_j\nu_k\nu_m$ for all combinations of i, j, k, m (= 1,2,3) and for all α. Initialize $\dot{\boldsymbol{\epsilon}}^I = \boldsymbol{\sigma}^I = \Delta\boldsymbol{\sigma} = \Delta\dot{\boldsymbol{\epsilon}} = \Delta\dot{\boldsymbol{\epsilon}}'' = \mathbf{0}$, in which $\boldsymbol{\sigma} = (\sigma_{11}, \sigma_{22}, \sigma_{33}, \sigma_{12}, \sigma_{23}, \sigma_{31})^T$ = column matrix of macroscopic stress components; $\dot{\boldsymbol{\epsilon}}$ = similar column matrix of strain-rate components; and $\dot{\boldsymbol{\epsilon}}''$ = column matrix of inelastic strain rates. Specify increment $\Delta\sigma_{11}$. Set $\boldsymbol{\sigma}^M = \boldsymbol{\sigma}^I + \Delta\boldsymbol{\sigma}/2$, $\boldsymbol{\sigma}^F = \boldsymbol{\sigma}^I + \Delta\boldsymbol{\sigma}$ (Superscripts I, M, and F refer to the initial, middle, and final values for the step.)
2. Loop on loading steps.
3. Iteration loop.
4. Compute from Eq. 11 $\boldsymbol{\beta}^M$ based on $\boldsymbol{\sigma}^M$, and $\boldsymbol{\beta}^F$ based on $\boldsymbol{\sigma}^F$. Compute $\Delta\boldsymbol{\beta} = \boldsymbol{\beta}^F - \boldsymbol{\beta}^I$ and $\Delta\dot{\boldsymbol{\epsilon}}'' = -\Delta\boldsymbol{\beta}\boldsymbol{\sigma}^M$, in which $\boldsymbol{\beta}$ = 6 × 6 matrix of components β_{ijkm} of the fluidity tensor. Now the equation $\Delta\dot{\boldsymbol{\epsilon}} = \boldsymbol{\beta}\,\Delta\boldsymbol{\sigma} - \Delta\dot{\boldsymbol{\epsilon}}''$ is a system of six linear algebraic equations, in which some unknowns are the $\Delta\dot{\boldsymbol{\epsilon}}$ components on the left-hand side, and other unknowns are the $\Delta\boldsymbol{\sigma}$ components on the right-hand side. These equations must be rearranged so that all unknowns are on the left-hand side. For our fitting of test data for clays, the value of $\Delta\sigma_{11}$ is specified; and $\Delta\sigma_{22} = \Delta\sigma_{33}$ (axisymmetric tests), $\Delta\sigma_{12} = \Delta\sigma_{13} = \Delta\sigma_{23} = 0$, and $\Delta\epsilon_{11} + \Delta\epsilon_{22} + \Delta\epsilon_{33} = 0$ (no volume change, since only deviatoric creep is modeled by the present theory). This amounts to six conditions and suffices to solve the unknowns $\Delta\sigma_{22}$, $\Delta\epsilon_{11}$, $\Delta\epsilon_{22}$, $\Delta\epsilon_{12}$, $\Delta\epsilon_{23}$, and $\Delta\epsilon_{31}$. Then update $\dot{\boldsymbol{\epsilon}}^F = \dot{\boldsymbol{\epsilon}}^I + \Delta\dot{\boldsymbol{\epsilon}}$, $\boldsymbol{\sigma}^F = \boldsymbol{\sigma}^I + \Delta\boldsymbol{\sigma}$, $\boldsymbol{\sigma}^M = \boldsymbol{\sigma}^I + \Delta\boldsymbol{\sigma}/2$ and reset the newly calculated values in $\Delta\boldsymbol{\sigma}$.
5. Iterate the steps 3–4 until the change of $\Delta\boldsymbol{\sigma}$ from the preceding iteration meets the given tolerance, such that the sum of the square of all stress changes is less than a given number. Print the results as needed.
6. Reset $\dot{\boldsymbol{\epsilon}}^I \leftarrow \dot{\boldsymbol{\epsilon}}^F$, $\boldsymbol{\sigma}^I \leftarrow \boldsymbol{\sigma}^F$, $\boldsymbol{\sigma}^F \leftarrow \boldsymbol{\sigma}^I + \Delta\boldsymbol{\sigma}$, $\boldsymbol{\sigma}^M \leftarrow \boldsymbol{\sigma}^I + \Delta\boldsymbol{\sigma}/2$. Then return to 2 to start a new loading step unless the final strain has been reached.

This algorithm can be used when the specimen is tranversely isotropic and is loaded along the axis of transverse isotropy. To speed up convergence, the foregoing algorithm may be modified by calculating new $\Delta\boldsymbol{\sigma}$ as $\tau\Delta\boldsymbol{\sigma}^{(i-1)} + (1 - \tau)\Delta\boldsymbol{\sigma}^{(i)}$ where superscripts i and $i - 1$ refer to the last two preceding iterations; and τ = an empirical parameter such that $0 < \tau \leq 1$.

The foregoing algorithm has been used to calculate the responses for various values of k_0 and k_2, in order to find, in a trial-and-error fashion, the k_1 and k_2 values that give the optimum fit of the test data.

Frequency Distribution of Orientations

The anisotropy of clay microstructure is geometrically characterized by the frequency distribution function $f(n)$ of the clay platelet orientations; $\mathbf{n} = (n_1, n_2, n_3)$ = unit normal to a clay platelet (2,11,29). In the previous work (6), it was assumed that the direction of interparticle slipping coincided with the direction of the clay platelets. This was, of course, a simplifying hypothesis. First, the plane of shear strain on the microplane need not exactly coincide with the direction of interparticle slipping, and second, typically we may imagine a tip or edge-to-plane contact of two platelets, in which case there is some ambiguity as to which of the two platelets represents the plane of slipping.

We introduce a different hypothesis, assuming that interparticle slipping is modeled by normal strains on the microplanes such that the direction of the normal strain rates is parallel to the clay platelet on which the slipping occurs; see Fig. 1. While, in the previous approach, the frequency distribution function $f(\mathbf{n})$ could be taken approximately as the distribution function for the initensity of shear strain rates on microplanes of various orientations, for our present hypothesis we need to modify this function to obtain the frequency distribution function $\Phi(\boldsymbol{\nu})$ for the distribution of the intensity of the normal strain rates as a function of slip orientations $\boldsymbol{\nu}$; $\boldsymbol{\nu} = (\nu_1, \nu_2, \nu_3)$ = unit vector (Fig. 2). In terms of the spherical coordinates (θ, ϕ) shown in Fig. 2, the unit vectors of microplane normals and of clay platelets are

$$\nu_1 = \cos\theta; \quad \nu_2 = \cos\phi \sin\theta; \quad \nu_3 = \sin\phi \sin\theta \quad \ldots\ldots\ldots\ldots\ldots\ldots \quad (13a)$$

$$n_1 = \cos\theta'; \quad n_2 = \cos\phi' \sin\theta'; \quad n_3 = \sin\phi' \sin\theta' \quad \ldots\ldots\ldots\ldots\ldots\ldots \quad (13b)$$

According to our hypothesis number 2, we may assume that slipping over all the clay platelets that are normal to the given microplane of orientation $\boldsymbol{\nu}$ makes the same contribution to the normal strain rate on this microplane. Therefore, we can calculate $\Phi(\boldsymbol{\nu})$ as the integral of $f(\mathbf{n})$ over a circle of radius 1 (Fig. 2) on the plane perpendicular to $\boldsymbol{\nu}$:

$$\Phi(\boldsymbol{\nu}) = k \int_\Gamma f(\mathbf{n}) ds' \quad \text{or} \quad \Phi(\theta, \phi) = k \int_\Gamma f(\theta', \phi') ds' \quad \ldots\ldots\ldots\ldots\ldots\ldots \quad (14)$$

in which Γ = the circumference of the unit circle; and k = a normalizing factor. Since $\boldsymbol{\nu} \perp \mathbf{n}$, i.e., $\boldsymbol{\nu} \cdot \mathbf{n} = 0$, we have $\cos\theta \cos\theta' + \cos\phi \sin\theta \cos\phi' \sin\theta' + \sin\phi \sin\theta \sin\phi' \sin\theta' = 0$, which may be rewritten as

$$G(\theta', \phi') = \cos\theta \cos\theta' + \cos(\phi - \phi') \sin\theta \sin\theta' = 0 \quad \ldots\ldots\ldots\ldots\ldots\ldots \quad (15)$$

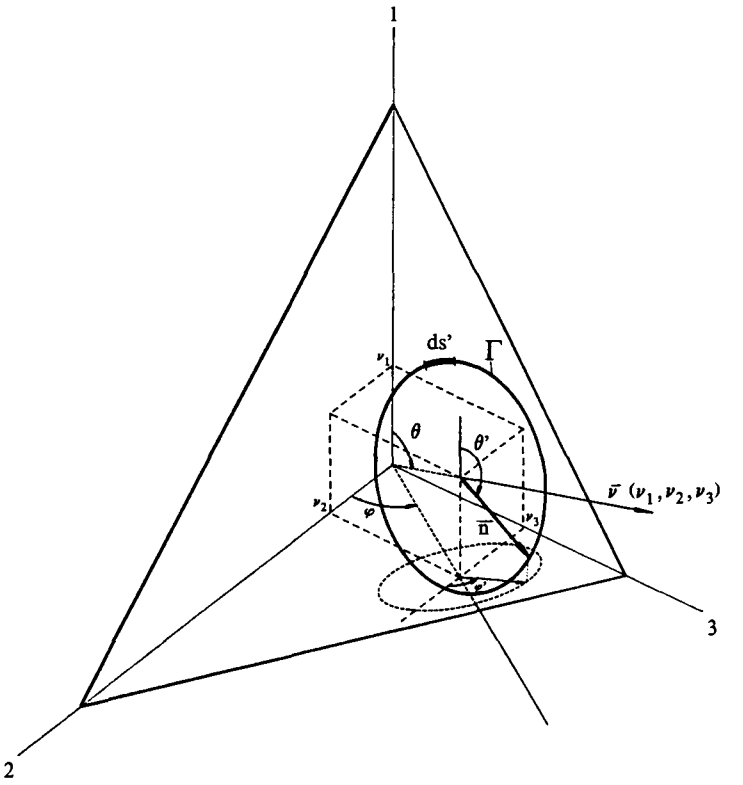

FIG. 2.—Slip Vector ν as Normal to Microplane; All Clay Platelets with Unit Normal n Perpendicular to ν Contribute to Slip in this Direction

This defines function $G(\theta', \phi')$.

Except for two special cases to be considered later, Eq. 15 provides a unique relation between θ' and ϕ', for each given pair (θ, ϕ), i.e., $\theta' = g(\phi')$. Hence

$$f(\theta', \phi') = f[g(\phi'), \phi'] = F(\phi') \quad \ldots\ldots\ldots\ldots\ldots\ldots\ldots\ldots\ldots\ldots \quad (16)$$

where $F(\phi')$ is introduced as a notation for this function. Also

$$ds' = (d\theta'^2 + \sin^2\theta' d\phi'^2)^{1/2} \quad \ldots\ldots\ldots\ldots\ldots\ldots\ldots\ldots\ldots\ldots \quad (17)$$

Furthermore, by differentiation of Eq. 15 we have $dG = (\partial G/\partial\theta')d\theta' + (\partial G/\partial\phi')d\phi' = 0$, from which

$$d\theta' = \frac{\dfrac{\partial G}{\partial \phi'}}{\dfrac{\partial G}{\partial \theta'}} d\phi' \quad \ldots\ldots\ldots\ldots\ldots\ldots\ldots\ldots\ldots\ldots\ldots\ldots \quad (18)$$

Finally, substituting Eqs. 16–18 into Eq. 14, we obtain

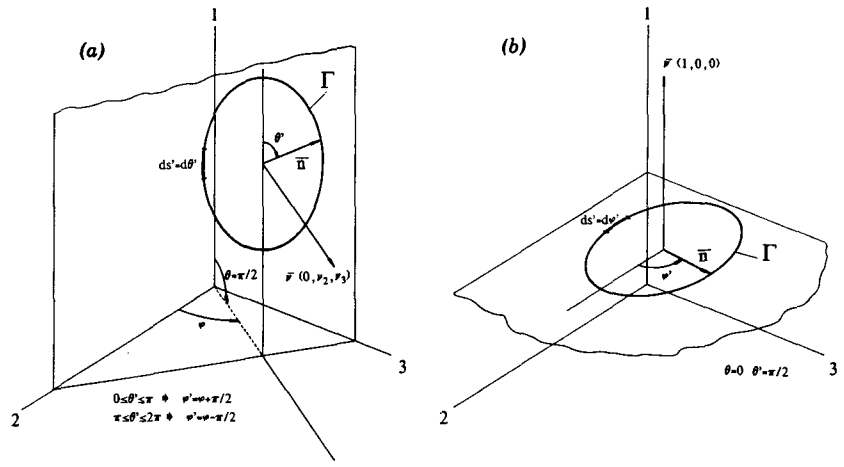

FIG. 3.—Special Cases: (*a*) Horizontal Slipping, $\theta = \pi/2$; (*b*) Vertical Slipping, $\theta = 0$

$$\Phi(\theta,\phi) = k\int_{-\pi}^{\pi} F(\phi')\left[\frac{\sin(\phi-\phi')\sin\theta\sin\theta'}{\cos(\phi-\phi')\sin\theta\cos\theta' - \cos\theta\sin\theta'}\right]^{1/2} d\phi' \quad \ldots\ldots (19)$$

The integrand of this equation is a function of ϕ' only because $\theta' = g(\phi')$. This integral is evaluated numerically. The normalizing factor is calculated from the condition (in which S denotes a unit hemisphere):

$$\int_S \Phi(\theta,\phi)\,dS = 1 \quad \ldots\ldots (20)$$

There are two special cases for which the foregoing calculation is impossible:

1. $\theta = \pi/2$ [Fig. 3(*a*)]. In this case, ϕ' is irrelevant; $d\phi' = 0$, $ds' = d\theta'$, $f(\theta',\phi') \equiv F(\theta')$, $\phi' = \phi \pm \pi/2$; and

$$\Phi(\theta,\phi) = \int_{-\pi}^{+\pi} f(\theta',\phi')\,d\theta' = \int_{-\pi}^{+\pi} F(\theta')\,d\theta' = 4\int_0^{\pi/2} F(\theta')\,d\theta' \quad \ldots\ldots (21)$$

2. $\theta = 0$ [Fig. 3(*b*)]. In this case, $ds' = d\theta'$, $\theta' = \pi/2$, and $\Phi(\theta,\phi) = \int_{-\pi}^{+\pi} f(\theta',\phi')\,d\theta' = \int_{-\pi}^{+\pi} F(\theta')\,d\theta'$. But $F(\theta') = F(90°) =$ constant, and so

$$\Phi(\theta,\phi) = 2\pi F(90°) \quad \ldots\ldots (22)$$

Comparison with Test Data

Figs. 4–8 show fits of various test data on deviatoric creep of anisotropic clays that are available in the literature (1,9,10,18,20,24,26). In some of these data, the frequency distribution function of clay platelet orientations has been measured by X-ray scattering (11) and is shown in

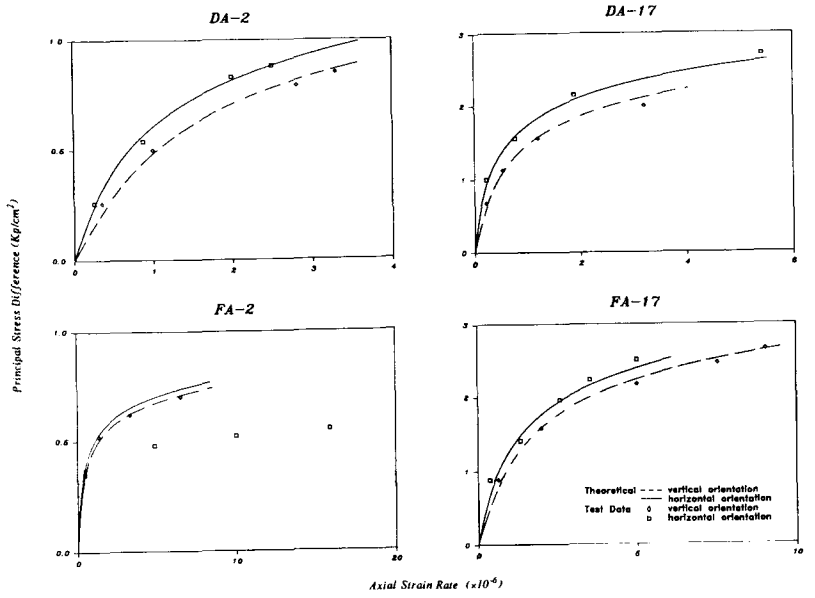

FIG. 4.—Comparison with Test Data for Anisotropically Consolidated Specimens (Bažant, et al.) 1,000 min after Loading

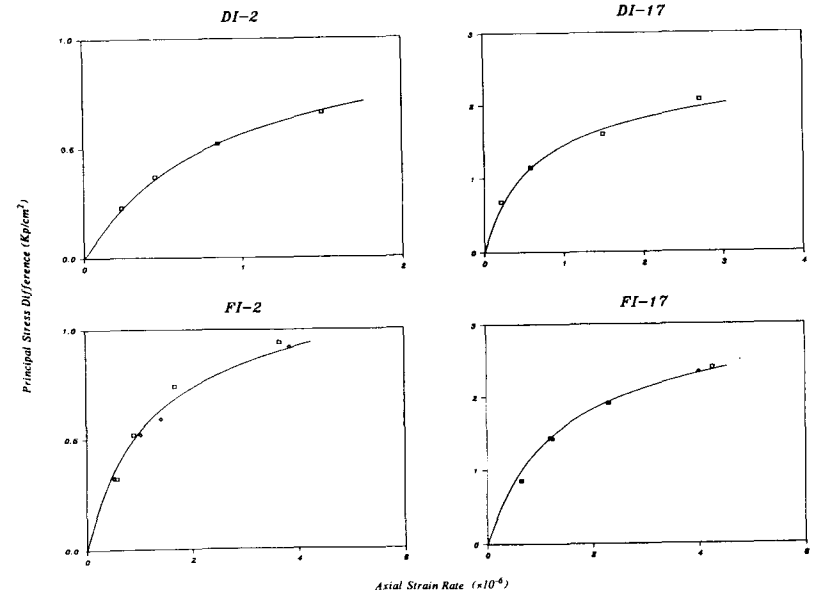

FIG. 5.—Comparison with Test Data for Isotropically Consolidated Specimens (Bažant, et al.) 1,000 min after Loading

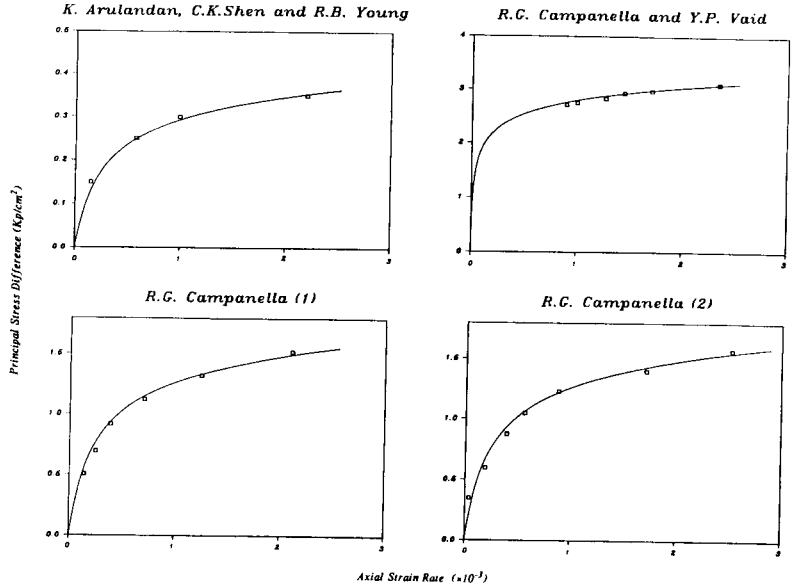

FIG. 6.—Comparison with Test Data for Isotropically Consolidated Specimens (Arulandan, et al.; Campanella and Vaid; Campanella) 1 min after Loading

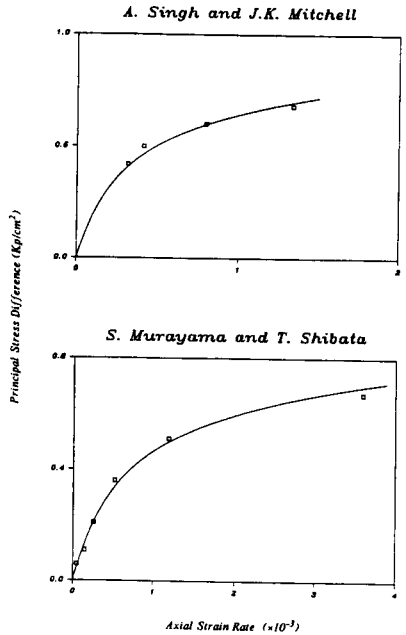

FIG. 7.—Comparison with Test Data for Isotropically Consolidated Specimens (Singh and Mitchell; Murayama and Shibata) 1 min after Loading

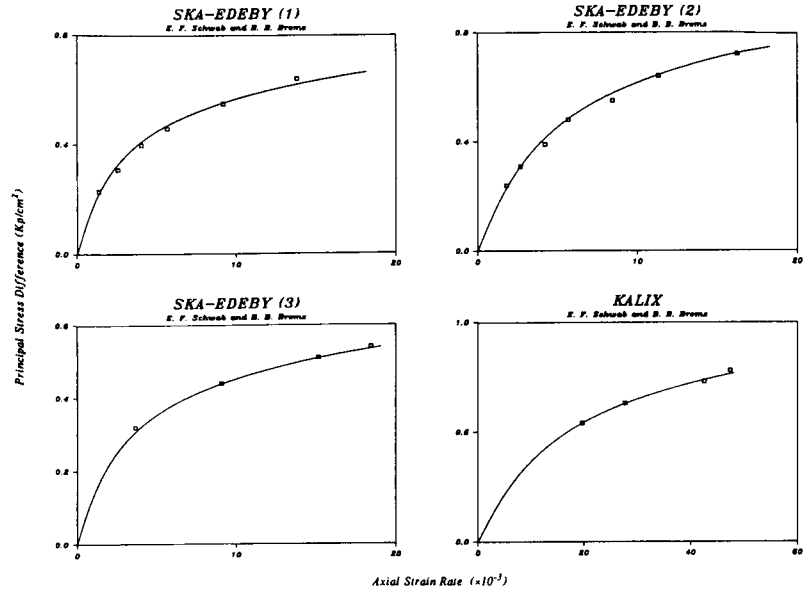

FIG. 8.—Comparison with Test Data from Field Vane Test (Schwab and Broms) 1 min after Loading

TABLE 1.—Optimum Material Parameters

Test data (1)	Time exponent (m) (2)	Stress level parameter, k_2 (mm²/N) (3)	Creep rate parameter, k_0 (mm/min) (4)
Bažant, et al.			
DA-2	0.77	110.0	1.00×10^{-4}
DA-17	0.72	59.0	1.88×10^{-4}
FA-2	1.00	220.0	0.19×10^{-4}
FA-17	0.86	47.5	2.00×10^{-4}
DI-2	0.82	135.0	0.80×10^{-4}
DI-17	0.80	62.0	1.85×10^{-4}
FI-2	1.00	120.0	1.00×10^{-4}
FI-17	0.90	47.0	4.20×10^{-4}
Murayama and Shibata	0.99	180.0	2.25×10^{-4}
Singh and Mitchell	0.83	168.0	1.10×10^{-4}
Campanella (1)	0.86	95.0	0.75×10^{-4}
Campanella (2)	0.86	95.0	0.75×10^{-4}
Campanella and Vaid	0.61	69.5	0.05×10^{-4}
Arulandan, et al.	0.80	395.0	0.85×10^{-4}
SKA-EDEBY (1)	0.88	195.0	1.00×10^{-3}
SKA-EDEBY (2)	0.89	175.0	1.75×10^{-3}
SKA-EDEBY (3)	0.73	235.0	1.15×10^{-3}
KALIX	0.84	135.0	6.00×10^{-3}

Fig. 2 of Ref. 6. Although such measurements are very difficult and might not yield a very accurate estimation of this distribution function, we nevertheless use it for the present calculation, considering it better than having no information at all on the distribution function.

Fig. 4 represents data for anisotropic clay obtained from Ref. 9. The clay specimens were prepared using the method developed by Edil (14), Krizek, et al. (16), and Sheeran and Krizek (25). Two kinds of specimens were obtained from the same anisotropically consolidated clay, one kind trimmed horizontally and another kind trimmed vertically. The values of $f(n)^{\alpha}$ are obtained from Ref. 11 and are used as explained earlier to compute the values of $\phi(\nu)^{\alpha}$.

Good agreement is found for all specimens except the specimen horizontally trimmed from sample FA-2, which exhibits excessively large deformation during creep. It is the opinion of the authors (9) that, since this was a very soft sample, the specimen was probably disturbed while setting up the test.

Figs. 5–7 exhibit comparison with test data for isotropically consolidated clays from Refs. 1, 9, 10, 18, and 26. Again, two kinds of specimens were used for the data set of Fig. 5, as described earlier. The actual frequency distribution $f(\mathbf{n})$ was not available and, therefore, true isotropy was assumed, i.e., $f(\mathbf{n}) = \phi(\boldsymbol{\nu}) = 1$.

Fig. 8 shows comparison with data from the vane test. Since no other information was available, isotropy was assumed for this data set. One can observe (Table 1) that the values of k_0 are much higher for these data than for the preceding ones. The reason is the way the strain rate is reported; the authors (24) used the average strain rate, i.e., the current strain divided by the current time.

Conclusions

1. The present microplane model for creep of anisotropic clays models interparticle slipping through normal strain rates on the microplanes. This is simpler than the previous microplane model (6), which described interparticle slipping by shear strain rates on the microplanes.
2. The present model based on normal strain rates on the microplanes describes material anisotropy correctly only if the microplanes are assumed to be statically constrained, i.e., the stress components on each microplane are the resolved components of the macroscopic stress tensor. This contrasts with the previous microplane model based on shear strain rates on the microplanes, for which material anisotropy was described correctly only if a kinematic constraint of the microplanes was used.
3. Material anisotropy is characterized by a distribution function for the normal strain rates, which can be approximately estimated from the frequency distribution function of the clay platelet orientations.
4. The fluidity matrix of anisotropic clay may be calculated from the principle of complementary virtual work, which expresses in the average sense the condition of compatibility of the strain rates on various microplanes.
5. The present calculations again confirm the previous conclusions that the creep rate of clay follows the activation energy concept (rate process theory).
6. The typical test data available in the literature can be described by the present model with a good accuracy.

Acknowledgments

Financial support under the United States National Science Foundation Grant No. CEE 821-1642 to Northwestern University is gratefully appreciated.

Appendix.—References

1. Arulanandan, K., Shen, C. K., and Young, R. B., "Undrained Creep Behaviour of a Coastal Organic Silty Clay," *Geotechnique*, Vol. 21, No. 4, 1971, pp. 359–375.
2. Baker, D. W., Wenk, A. R., and Christie, J. M., "X-ray Analysis of Preferred Orientation in Fine Grained Quartz Aggregates," *Journal of Geology*, Vol. 77, 1969, pp. 144–172.
3. Batdorf, S. B., and Budianski, B., "A Mathematical Theory of Plasticity Based on the Concept of Slip," *National Advisory Committee for Aeronautics (N.A.C.A.), Technical Note No. 1871*, Washington, D.C., Apr., 1949.
4. Bažant, Z. P., and Oh, B. H., "Microplane Model for Progressive Fracture of Concrete and Rock," *Journal of Engineering Mechanics*, ASCE, Vol. 111, No. 4, Apr., 1985, pp. 559–582.
5. Bažant, Z. P., and Oh, B. H., "Efficient Numerical Integration on the Surface of a Sphere," *Zeitschrift für Angewandte Mathematik und Mechanik (ZAMM)*, Vol. 66, 1986, No. 1, pp. 37–49.
6. Bažant, Z. P., and Kim, J. K., "Creep of Anisotropic Clay: Microplane Model," *Journal of Geotechnical Engineering*, ASCE, Vol. 112, No. 4, Apr., 1986, pp. 458–475.
7. Bažant, Z. P., and Oh, B. H., "Microplane Model for Fracture Analysis of Concrete Structures," *Proceedings*, Symposium on the Interaction of Non-nuclear Munitions with Structures," U.S. Air Force Academy, Colorado Springs, Colo., May, 1983, pp. 49–55.
8. Bažant, Z. P., "Microplane Model for Strain-Controlled Inelastic Behavior," Chapter 3, *Mechanics of Engineering Materials*, C. S. Desai and R. H. Gallagher, Eds., John Wiley & Sons, New York, N.Y., 1984, pp. 45–59.
9. Bažant, Z. P., and Ozaydin, K., and Krizek, R. J., "Micromechanics Model for Creep of Anisotropic Clay," *Journal of the Engineering Mechanics Division*, ASCE, Vol. 101, No 1, Feb., 1975, pp. 57–78.
10. Campanella, R. G., and Vaid, Y. P., "Triaxial and Plane Strain Creep Rupture of an Undisturbed Clay," *Canadian Geotechnical Journal*, Vol. 11, No. 1, Feb., 1974, pp. 1–10.
11. Chawla, K. N., "Effect of Fabric on Creep Response of Kaolinite Clay," thesis presented to Northwestern University, at Evanston, Ill., in 1973, in partial fulfillment of the requirements for the degree of Doctor of Philosophy.
12. Christensen, R. W., and Wu, T. H., "Analysis of Clay Deformation as a Rate Process," *Journal of the Soil Mechanics and Foundations Division*, ASCE, Vol. 90, No. 6, Nov., 1964, pp. 125–127.
13. Cottrell, A. H., *The Mechanical Properties of Matter*, John Wiley & Sons, Inc., New York, N.Y., 1964.
14. Edil, T. B., "Influence of Fabric and Soil Water Potential on Stress-Strain Response of Clay," thesis presented to Northwestern University, at Evanston, Ill., in 1973, in partial fulfillment of the requirements for the degree of Doctor of Philosophy.
15. Glasstone, S., Laidler, K. J., and Eyring, H., *The Theory of Rate Processes*, McGraw-Hill Book Co., Inc., New York, N.Y., 1941.

16. Krizek, R. J., Edil, T. B., and Ozaydin, I. K., "Preparation and Identification of Clay Samples with Controlled Fabric," *Engineering Geology*, 1975, Vol. 9, pp. 13–38.
17. Mitchell, J. K., "Shearing Resistance of Soils as a Rate Process," *Journal of the Soil Mechanics and Foundations Division*, ASCE, Vol. 90, No. 1, Jan., 1964, pp. 29–61.
18. Mitchell, J. K., Campanella, R. G., and Singh, A., "Soil Creep as a Rate Process," *Journal of the Soil Mechanics and Foundations Division*, ASCE, Vol. 94, No. 1, Jan., 1968, pp. 231–253.
19. Murayama, S., and Shibata, T., "On the Rheological Character of Clay," *Transactions of the Japan Society of Civil Engineers*, Vol. 19, No. 40, pp. 1–31.
20. Murayama, S., and Shibata, T., "Rheological Properties of Clays," *Proceedings*, 5th International Congress on Soil Mechanics and Engineering Foundations, Paris, France, 1961, pp. 269–273.
21. Murayama, S., and Shibata, T., "Flow and Stress Relaxation of Clays (Rheology and Soil Mechanics)," *Proceedings*, Symposium on Rheology and Soil Mechanics, International Union of Theoretical and Applied Mechanics, Grenoble, France, Apr., 1964, pp. 99–129.
22. Pande, G. H., and Sharma, K. G., "Multi-Laminate Model of Clays—A Numerical Evaluation of the Influence of Rotation of the Principal Stress Axes," *Report*, Dept. of Civil Engineering, University College of Swansea, U.K., 1982.
23. Pande, G. N., and Sharma, K. G., "A Micro-Structural Model for Soils under Cyclic Loading," International Symposium on Soils under Cyclic and Transient Loading, Swansea, U.K., Jan., 1980, pp. 451–462.
24. Schwab, E. F., and Broms, B. B., "Pressure-Settlement-Time Relationship by Screw Plate Tests in Situ," *9th International Conference on Soil Mechanics and Foundation Engineering*, Vol. 1, Tokyo, Japan, 1977, pp. 281–288.
25. Sheeran, D. E., and Krizek, R. J., "Preparation of Homogeneous Soil Sampling by Slurry Consolidation," *Journal of Materials*, American Society for Testing and Materials, Vol. 6, 1971, pp. 356–373.
26. Singh, A., and Mitchell, J. K., "General Stress-Strain-Time Function for Soils," *Journal of the Soil Mechanics and Foundations Division*, ASCE, Vol. 94, No. 1, Jan., 1968, pp. 21–26.
27. Stroud, A. H., *Approximate Calculation of Multiple Integrals*, Prentice Hall, Englewood Cliffs, N.J., 1971.
28. Taylor, G. I., "Plastic Strain in Metals," *Journal of the Institute of Metals*, Vol. 62, 1938, pp. 307–324.
29. Tullis, T. E., "Experimental Development of Preferred Orientation of Mica During Recrystallization," thesis presented to the University of California, at Los Angeles, Calif., in 1971, in partial fulfillment of the requirements for the degree of Doctor of Philosophy.
30. Vaid, Y. P., and Campanella, R. G., "Time-Dependent Behaviour of Undrained Clay," *Journal of the Geotechnical Engineering Division*, ASCE, Vol. 103, No. 7, Jul., 1977, pp. 693–709.
31. Wu, T. Y., Resendiz, D., and Neukirchner, R. J., "Analysis of Consolidation by Rate Process Theory," *Journal of he Soil Mechanics and Foundations Division*, ASCE, Vol. 92, No. 6, Nov., 1966, pp. 229–248.